

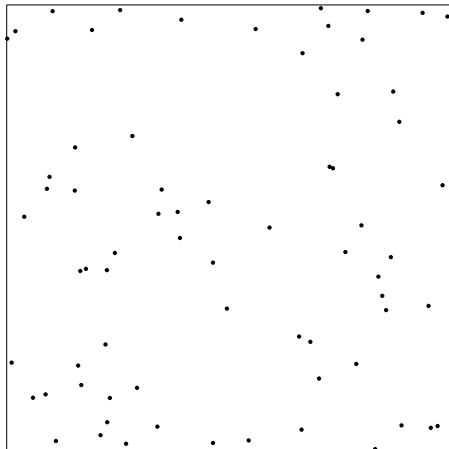
The accumulated persistence function, a useful functional
summary statistic for topological data analysis

Christophe A. N. Biscio and Jesper Møller, Aalborg University

May 15, 2017

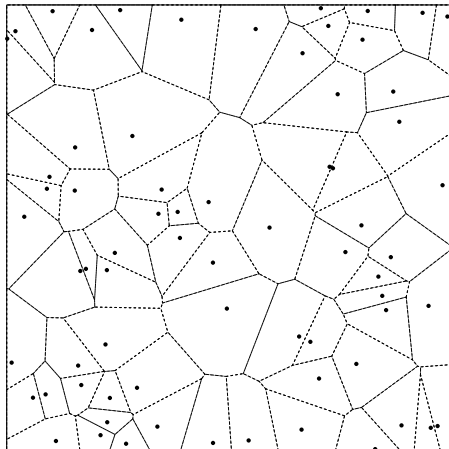
The case of a point cloud - Delaunay complex filtration

- Topological data analysis recovers the topological information from a spatial point process \mathbf{X} .



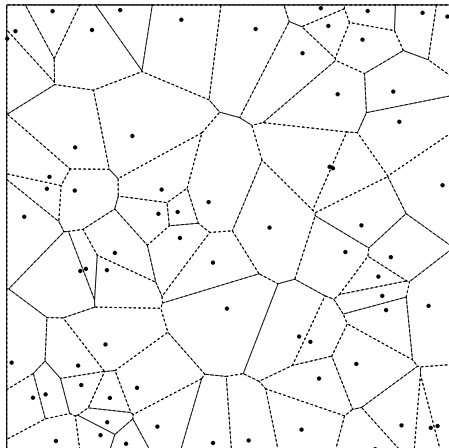
The case of a point cloud - Delaunay complex filtration

- Topological data analysis recovers the topological information from a spatial point process \mathbf{X} .
- Construct a so-called Delaunay complex filtration \sim union of growing balls of radius $r \geq 0$ intersected with the Voronoi tessellation...



The case of a point cloud - Delaunay complex filtration

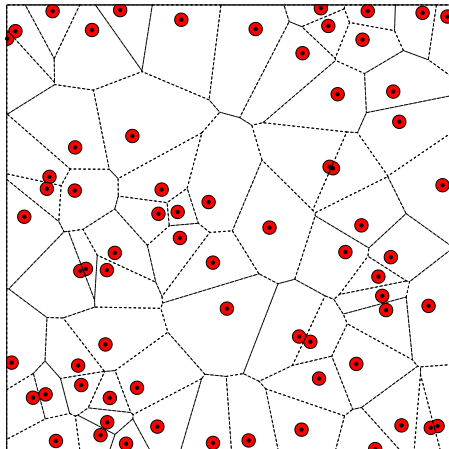
- Topological data analysis recovers the topological information from a spatial point process \mathbf{X} .
- Construct a so-called Delaunay complex filtration \sim union of growing balls of radius $r \geq 0$ intersected with the Voronoi tessellation...



- $r = 0$, each point represents the birth of a connected component.

The case of a point cloud - Delaunay complex filtration

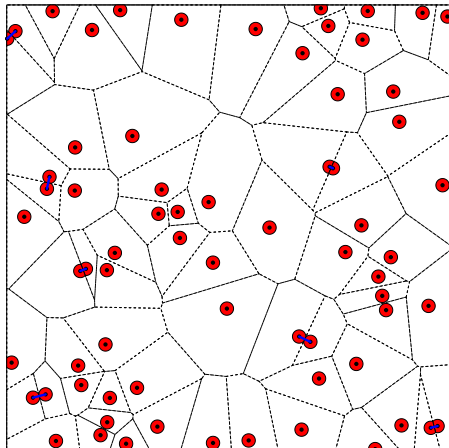
- Topological data analysis recovers the topological information from a spatial point process \mathbf{X} .
- Construct a so-called Delaunay complex filtration \sim union of growing balls of radius $r \geq 0$ intersected with the Voronoi tessellation...



- $r = 0$, each point represents the birth of a connected component.
- As r grows balls intersect...

The case of a point cloud - Delaunay complex filtration

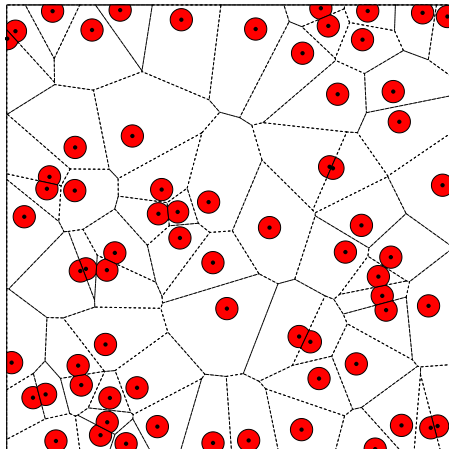
- Topological data analysis recovers the topological information from a spatial point process \mathbf{X} .
- Construct a so-called Delaunay complex filtration \sim union of growing balls of radius $r \geq 0$ intersected with the Voronoi tessellation...



- $r = 0$, each point represents the birth of a connected component.
- As r grows balls intersect...
- meaning that some connected components die/Delaunay edges appear.

The case of a point cloud - Delaunay complex filtration

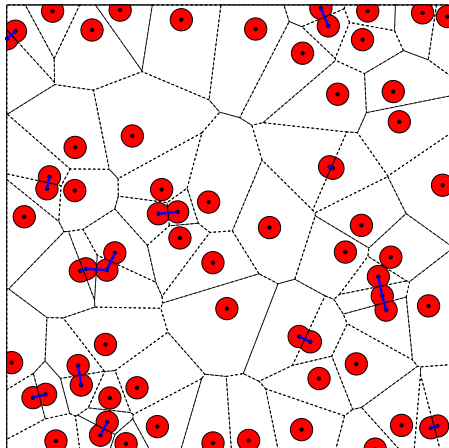
- Topological data analysis recovers the topological information from a spatial point process \mathbf{X} .
- Construct a so-called Delaunay complex filtration \sim union of growing balls of radius $r \geq 0$ intersected with the Voronoi tessellation...



- $r = 0$, each point represents the birth of a connected component.
- As r grows balls intersect...
- meaning that some connected components die/Delaunay edges appear.
- And so on as r grows...

The case of a point cloud - Delaunay complex filtration

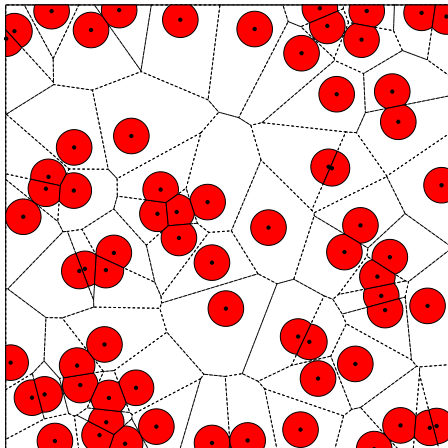
- Topological data analysis recovers the topological information from a spatial point process \mathbf{X} .
- Construct a so-called Delaunay complex filtration \sim union of growing balls of radius $r \geq 0$ intersected with the Voronoi tessellation...



- $r = 0$, each point represents the birth of a connected component.
- As r grows balls intersect...
- meaning that some connected components die/Delaunay edges appear.
- And so on as r grows...

The case of a point cloud - Delaunay complex filtration

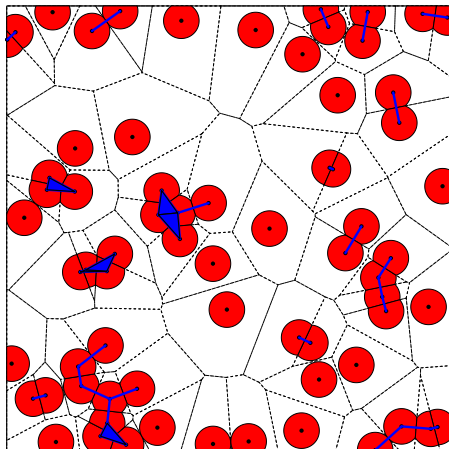
- Topological data analysis recovers the topological information from a spatial point process \mathbf{X} .
- Construct a so-called Delaunay complex filtration \sim union of growing balls of radius $r \geq 0$ intersected with the Voronoi tessellation...



- $r = 0$, each point represents the birth of a connected component.
- As r grows balls intersect...
- meaning that some connected components die/Delaunay edges appear.
- And so on as r grows...

The case of a point cloud - Delaunay complex filtration

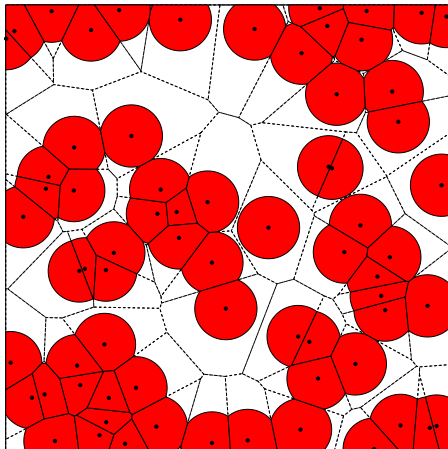
- Topological data analysis recovers the topological information from a spatial point process \mathbf{X} .
- Construct a so-called Delaunay complex filtration \sim union of growing balls of radius $r \geq 0$ intersected with the Voronoi tessellation...



- $r = 0$, each point represents the birth of a connected component.
- As r grows balls intersect...
- meaning that some connected components die/Delaunay edges appear.
- And so on as r grows...

The case of a point cloud - Delaunay complex filtration

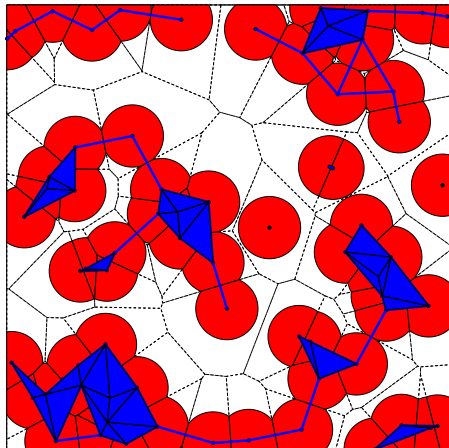
- Topological data analysis recovers the topological information from a spatial point process \mathbf{X} .
- Construct a so-called Delaunay complex filtration \sim union of growing balls of radius $r \geq 0$ intersected with the Voronoi tessellation...



- $r = 0$, each point represents the birth of a connected component.
- As r grows balls intersect...
- meaning that some connected components die/Delaunay edges appear.
- And so on as r grows...
- Also holes may appear (birth).

The case of a point cloud - Delaunay complex filtration

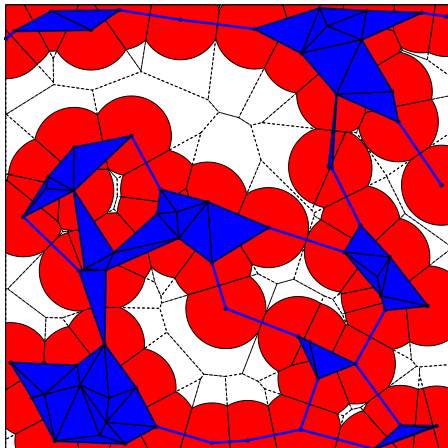
- Topological data analysis recovers the topological information from a spatial point process \mathbf{X} .
- Construct a so-called Delaunay complex filtration \sim union of growing balls of radius $r \geq 0$ intersected with the Voronoi tessellation...



- $r = 0$, each point represents the birth of a connected component.
- As r grows balls intersect...
- meaning that some connected components die/Delaunay edges appear.
- And so on as r grows...
- Also holes may appear (birth).

The case of a point cloud - Delaunay complex filtration

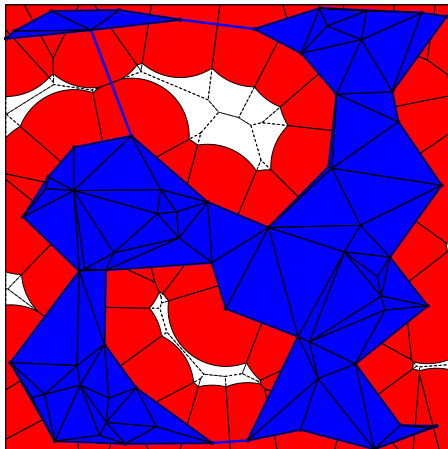
- Topological data analysis recovers the topological information from a spatial point process \mathbf{X} .
- Construct a so-called Delaunay complex filtration \sim union of growing balls of radius $r \geq 0$ intersected with the Voronoi tessellation...



- $r = 0$, each point represents the birth of a connected component.
- As r grows balls intersect...
- meaning that some connected components die/Delaunay edges appear.
- And so on as r grows...
- Also holes may appear (birth).
- And holes may disappear (death).

The case of a point cloud - Delaunay complex filtration

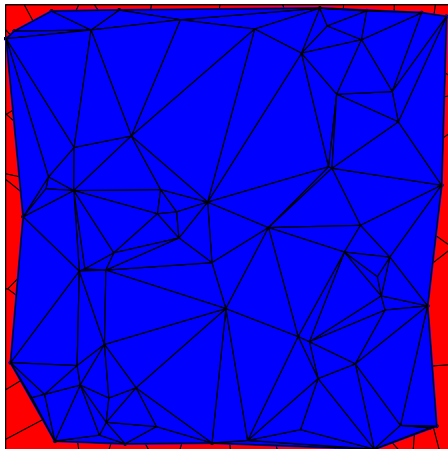
- Topological data analysis recovers the topological information from a spatial point process \mathbf{X} .
- Construct a so-called Delaunay complex filtration \sim union of growing balls of radius $r \geq 0$ intersected with the Voronoi tessellation...



- $r = 0$, each point represents the birth of a connected component.
- As r grows balls intersect...
- meaning that some connected components die/Delaunay edges appear.
- And so on as r grows...
- Also holes may appear (birth).
- And holes may disappear (death).

The case of a point cloud - Delaunay complex filtration

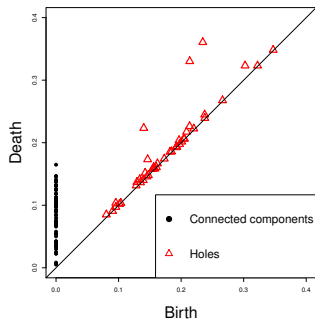
- Topological data analysis recovers the topological information from a spatial point process \mathbf{X} .
- Construct a so-called Delaunay complex filtration \sim union of growing balls of radius $r \geq 0$ intersected with the Voronoi tessellation...



- $r = 0$, each point represents the birth of a connected component.
- As r grows balls intersect...
- meaning that some connected components die/Delaunay edges appear.
- And so on as r grows...
- Also holes may appear (birth).
- And holes may disappear (death).

Main tool in persistent homology: Persistence diagram

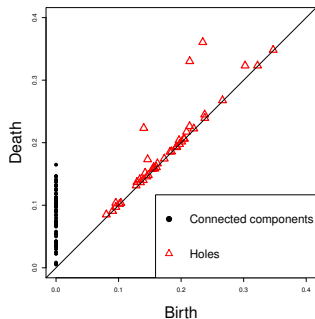
- For dimension $k = 0, 1, \dots$, a persistent diagram consists of points (b_i, d_i) representing as r varies connected components ($k = 0$), holes ($k = 1$), etc. appearing at $r = b_i$ (birth) and disappearing at $r = d_i$ (death),
- possibly with multiplicity c_i for (b_i, d_i) .



- Chazal et al. (2013), Chen et al. (2015)...: Difficult to apply statistical methods.

Main tool in persistent homology: Persistence diagram

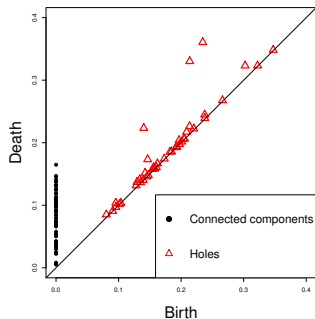
- For dimension $k = 0, 1, \dots$, a persistent diagram consists of points (b_i, d_i) representing as r varies connected components ($k = 0$), holes ($k = 1$), etc. appearing at $r = b_i$ (birth) and disappearing at $r = d_i$ (death),
- possibly with multiplicity c_i for (b_i, d_i) .



- Chazal et al. (2013), Chen et al. (2015)...: Difficult to apply statistical methods.
- Two-dim. alternatives: persistent landscape (Bubenik, 2015: sequence of 1-dim. functions).

Main tool in persistent homology: Persistence diagram

- For dimension $k = 0, 1, \dots$, a persistent diagram consists of points (b_i, d_i) representing as r varies connected components ($k = 0$), holes ($k = 1$), etc. appearing at $r = b_i$ (birth) and disappearing at $r = d_i$ (death),
- possibly with multiplicity c_i for (b_i, d_i) .



- Chazal et al. (2013), Chen et al. (2015)...: Difficult to apply statistical methods.
- Two-dim. alternatives: persistent landscape (Bubenik, 2015: sequence of 1-dim. functions).
- One-dim. alternatives provide selected information: Bubenik's dominant function λ_1 ; the silhouette (Chazal et al., 2013: a weighted average of Bubenik's functions); kernel estimate of the intensity function for the persistent diagram (Chen et al., 2015).

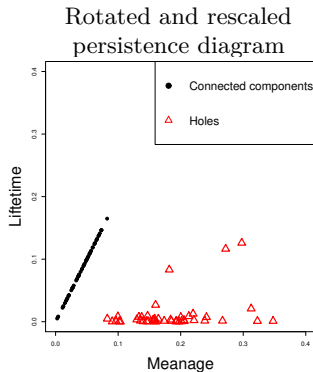
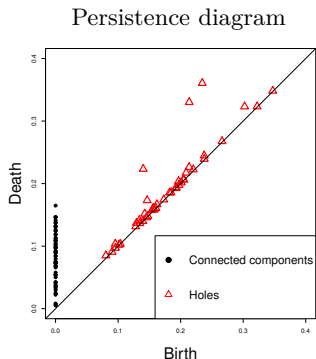
A new functional summary statistic

Uses the rotated and rescaled persistence diagram:

A new functional summary statistic

Uses the rotated and rescaled persistence diagram:

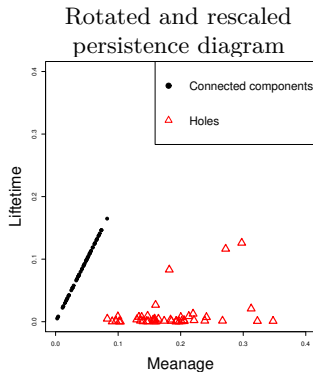
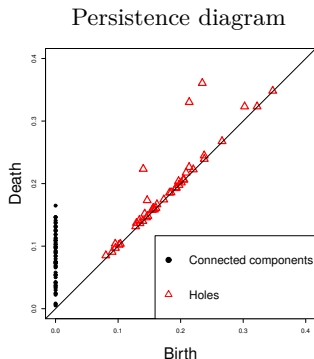
- $(b_i, d_i) \leftrightarrow (m_i, l_i)$, where
 $m_i = \frac{b_i + d_i}{2}$ is the meanage and
 $l_i = d_i - b_i$ is the lifetime.



A new functional summary statistic

Uses the rotated and rescaled persistence diagram:

- $(b_i, d_i) \leftrightarrow (m_i, l_i)$, where
 $m_i = \frac{b_i + d_i}{2}$ is the meanage and
 $l_i = d_i - b_i$ is the lifetime.



NB: For each dimension k , $PD_k \leftrightarrow RRPD_k$
(where $k = 0$ if connected components are considered, $k = 1$ if holes, $k = 2$ if voids...).

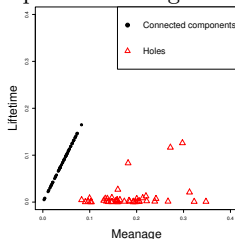
A new functional summary statistic

The **accumulated persistence function** for k -dimensional topological features:

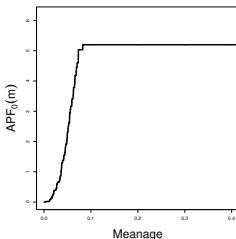
$$\text{APF}_k(m) = \sum_i c_i l_i \mathbf{1}(m_i \leq m), \quad m \geq 0.$$

Example:

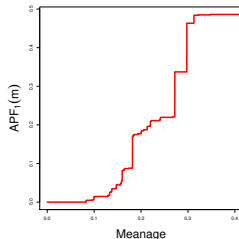
Rotated and rescaled
persistent diagram



Connected components



Holes



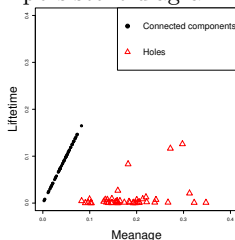
A new functional summary statistic

The **accumulated persistence function** for k -dimensional topological features:

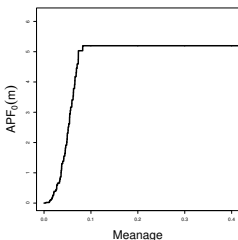
$$\text{APF}_k(m) = \sum_i c_i l_i \mathbf{1}(m_i \leq m), \quad m \geq 0.$$

Example:

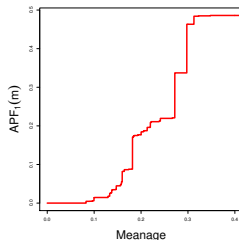
Rotated and rescaled
persistent diagram



Connected components



Holes



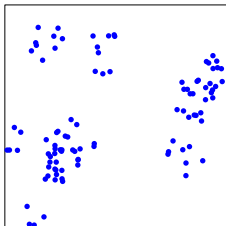
Under mild conditions, $\text{RRPD}_k \leftrightarrow \text{APF}_k$.

NB: APF_k is a 1-dim. function! Apply methods from functional data analysis...

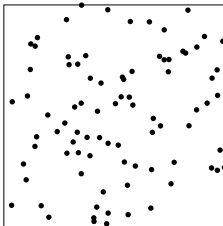
- A single APF:
 - Transfer confidence region for the persistence diagram to the APF
 - Extreme rank envelope
- A sample of APFs:
 - Functional boxplot
 - Confidence region for the mean of APFs
- Two or more samples of APFs:
 - Two-sample test
 - Clustering
 - Supervised classification

APFs for aggregated, completely random or regular point clouds

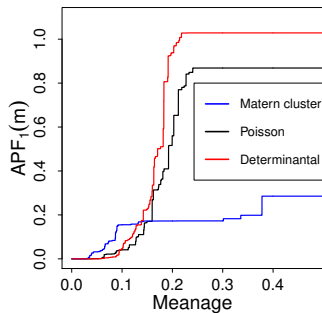
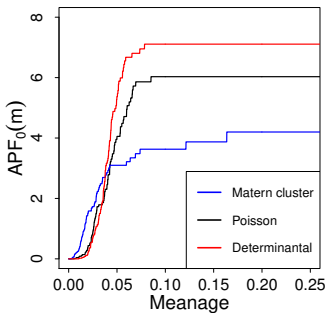
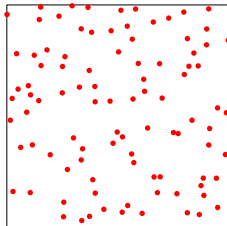
Matérn cluster



Poisson/CSR



Determinantal



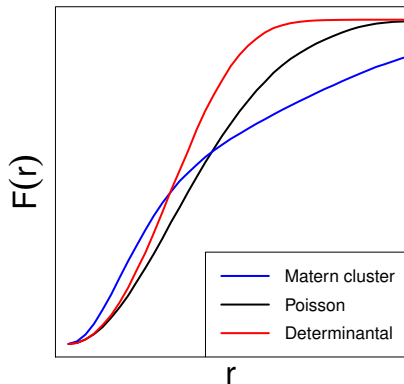
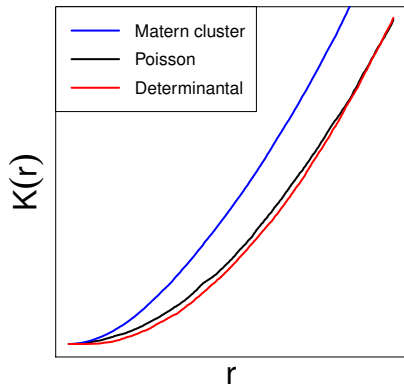
Classical functional summary functions for aggregated, completely random or regular point clouds

- Ripley's K -function for a stationary point process $X \subset \mathbb{R}^2$:

$$K(r) = \frac{E[\text{"Number of further points in } B(0, r)\text{"} \mid 0 \in \mathbf{X}]}{E[\text{"Number of points per unit area"}]}, \quad r \geq 0.$$

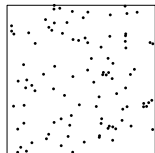
- The empty space function:

$$F(r) = P(\mathbf{X} \cap B(0, r) \neq \emptyset), \quad r \geq 0.$$

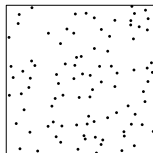


Extreme rank envelope test for CSR

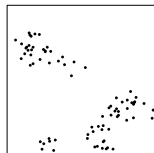
CSR: Poisson process



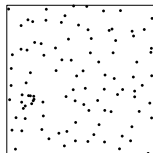
Inhibition: DPP



Aggregation:
Matérn cluster



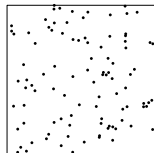
Baddeley-Silverman
cell process



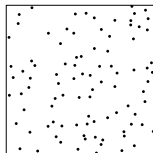
- Suppose each observed point cloud is modelled by $X \sim \text{Poisson}(\rho, [0, 1]^2)$, the Poisson point process on $[0, 1]^2$ with **known** intensity ρ ($= 100, 400$).

Extreme rank envelope test for CSR

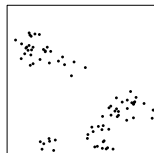
CSR: Poisson process



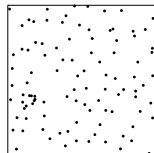
Inhibition: DPP



Aggregation:
Matérn cluster



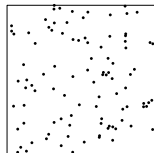
Baddeley-Silverman
cell process



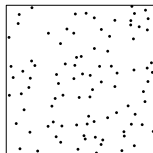
- Suppose each observed point cloud is modelled by $X \sim \text{Poisson}(\rho, [0, 1]^2)$, the Poisson point process on $[0, 1]^2$ with **known** intensity ρ ($= 100, 400$).
- Following Myllymäki *et al.* (2016): Simulate 2499 independent realizations from $\text{Poisson}(\rho, [0, 1]^2)$.

Extreme rank envelope test for CSR

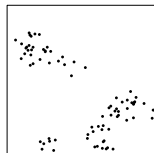
CSR: Poisson process



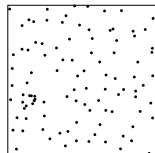
Inhibition: DPP



Aggregation:
Matérn cluster



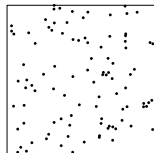
Baddeley-Silverman
cell process



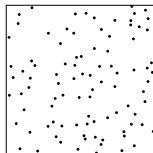
- Suppose each observed point cloud is modelled by $X \sim \text{Poisson}(\rho, [0, 1]^2)$, the Poisson point process on $[0, 1]^2$ with **known** intensity ρ ($= 100, 400$).
- Following Myllymäki *et al.* (2016): Simulate 2499 independent realizations from $\text{Poisson}(\rho, [0, 1]^2)$.
- In each of the 4 cases, given a functional summary statistic $(\text{APF}_0, \text{APF}_1, \hat{K}, \hat{F})$, compute extreme rank envelope test at level 5% (Myllymäki *et al.*, 2016).

Extreme rank envelope test for CSR

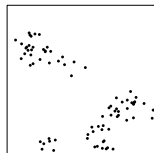
CSR: Poisson process



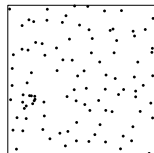
Inhibition: DPP



Aggregation:
Matérn cluster

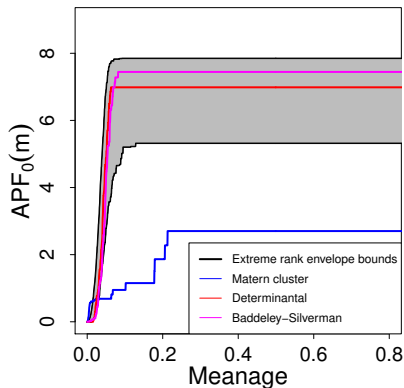


Baddeley-Silverman
cell process

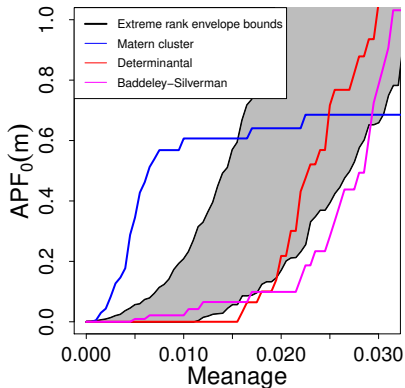


- Suppose each observed point cloud is modelled by $X \sim \text{Poisson}(\rho, [0, 1]^2)$, the Poisson point process on $[0, 1]^2$ with **known** intensity ρ ($= 100, 400$).
- Following Myllymäki *et al.* (2016): Simulate 2499 independent realizations from $\text{Poisson}(\rho, [0, 1]^2)$.
- In each of the 4 cases, given a functional summary statistic $(\text{APF}_0, \text{APF}_1, \hat{K}, \hat{F})$, compute extreme rank envelope test at level 5% (Myllymäki *et al.*, 2016).
- We repeated all this 500 times.

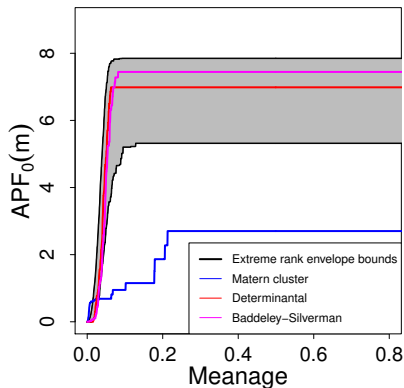
APF_0 in a case of rejection



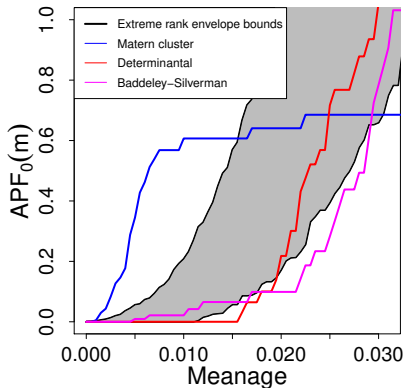
Zoom at 0



APF_0 in a case of rejection

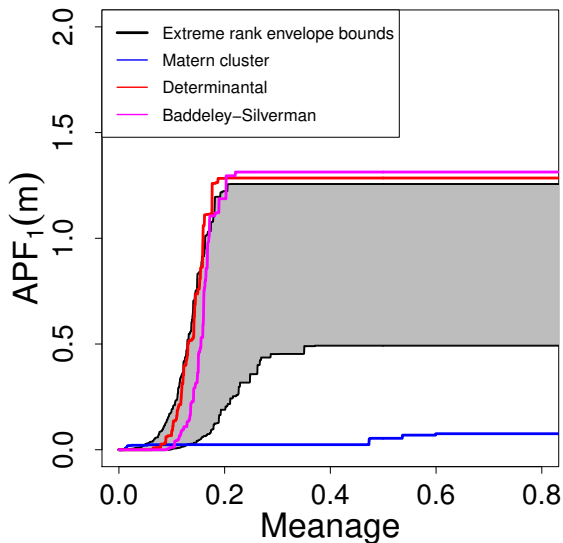


Zoom at 0



NB: Small lifetimes are not noise but of particular importance!

APF_1 in a case of rejection



Test for CSR using different functional summary statistics

Percentage of simulated point patterns rejected by the 95%-extreme rank envelope test.

	Poisson		Determinantal		Matérn cluster		Baddeley-Silverman	
	$\rho = 100$	$\rho = 400$	$\rho = 100$	$\rho = 400$	$\rho = 100$	$\rho = 400$	$\rho = 100$	$\rho = 400$
APF_0	3.6	4	77.4	100	100	100	45.6	99.6
APF_1	3.8	4.6	28.2	57.8	100	100	65.8	100
\hat{K}	3.4	2.8	97.4	100	100	100	52.4	50.2
\hat{F}	2.2	0.8	29.8	48.8	100	100	60.8	100
$APF_0, APF_1, \hat{K}, \hat{F}$	4.5	5	99	100	100	100	65	100

- Conservative test.

Test for CSR using different functional summary statistics

Percentage of simulated point patterns rejected by the 95%-extreme rank envelope test.

	Poisson		Determinantal		Matérn cluster		Baddeley-Silverman	
	$\rho = 100$	$\rho = 400$	$\rho = 100$	$\rho = 400$	$\rho = 100$	$\rho = 400$	$\rho = 100$	$\rho = 400$
APF_0	3.6	4	77.4	100	100	100	45.6	99.6
APF_1	3.8	4.6	28.2	57.8	100	100	65.8	100
\hat{K}	3.4	2.8	97.4	100	100	100	52.4	50.2
\hat{F}	2.2	0.8	29.8	48.8	100	100	60.8	100
$APF_0, APF_1, \hat{K}, \hat{F}$	4.5	5	99	100	100	100	65	100

- Conservative test.
- Good detection for inhibitive model when considered APF_0 and \hat{K} .

Test for CSR using different functional summary statistics

Percentage of simulated point patterns rejected by the 95%-extreme rank envelope test.

	Poisson		Determinantal		Matérn cluster		Baddeley-Silverman	
	$\rho = 100$	$\rho = 400$	$\rho = 100$	$\rho = 400$	$\rho = 100$	$\rho = 400$	$\rho = 100$	$\rho = 400$
APF_0	3.6	4	77.4	100	100	100	45.6	99.6
APF_1	3.8	4.6	28.2	57.8	100	100	65.8	100
\hat{K}	3.4	2.8	97.4	100	100	100	52.4	50.2
\hat{F}	2.2	0.8	29.8	48.8	100	100	60.8	100
$APF_0, APF_1, \hat{K}, \hat{F}$	4.5	5	99	100	100	100	65	100

- Conservative test.
- Good detection for inhibitive model when considered APF_0 and \hat{K} .
- Excellent detection for cluster model.

Test for CSR using different functional summary statistics

Percentage of simulated point patterns rejected by the 95%-extreme rank envelope test.

	Poisson		Determinantal		Matérn cluster		Baddeley-Silverman	
	$\rho = 100$	$\rho = 400$	$\rho = 100$	$\rho = 400$	$\rho = 100$	$\rho = 400$	$\rho = 100$	$\rho = 400$
APF_0	3.6	4	77.4	100	100	100	45.6	99.6
APF_1	3.8	4.6	28.2	57.8	100	100	65.8	100
\hat{K}	3.4	2.8	97.4	100	100	100	52.4	50.2
\hat{F}	2.2	0.8	29.8	48.8	100	100	60.8	100
$APF_0, APF_1, \hat{K}, \hat{F}$	4.5	5	99	100	100	100	65	100

- Conservative test.
- Good detection for inhibitive model when considered APF_0 and \hat{K} .
- Excellent detection for cluster model.
- Decent detection for Baddeley-Silverman cell process.

Test for CSR using different functional summary statistics

Percentage of simulated point patterns rejected by the 95%-extreme rank envelope test.

	Poisson		Determinantal		Matérn cluster		Baddeley-Silverman	
	$\rho = 100$	$\rho = 400$	$\rho = 100$	$\rho = 400$	$\rho = 100$	$\rho = 400$	$\rho = 100$	$\rho = 400$
APF_0	3.6	4	77.4	100	100	100	45.6	99.6
APF_1	3.8	4.6	28.2	57.8	100	100	65.8	100
\hat{K}	3.4	2.8	97.4	100	100	100	52.4	50.2
\hat{F}	2.2	0.8	29.8	48.8	100	100	60.8	100
$APF_0, APF_1, \hat{K}, \hat{F}$	4.5	5	99	100	100	100	65	100

- Conservative test.
- Good detection for inhibitive model when considered APF_0 and \hat{K} .
- Excellent detection for cluster model.
- Decent detection for Baddeley-Silverman cell process.
- The power increases with the number of points and by combining all summary statistics.

- A single APF
 - Transfer confidence region for the persistence diagram to the APF
 - Extreme rank envelope
- A sample of APFs
 - Functional boxplot
 - Confidence region for the mean of APFs
- Two or more samples of APFs
 - Two-sample test
 - Clustering
 - Supervised classification

Two-sample test

- D_0 and E_0 : two independent random rotated and rescaled persistence diagrams.

Two-sample test

- D_0 and E_0 : two independent random rotated and rescaled persistence diagrams.
- First sample is r_1 IID copies of D_0 : D_1, \dots, D_{r_1} .
- Second sample is r_2 IID copies of E_0 : E_1, \dots, E_{r_2} .
- $r = r_1 + r_2$ and A_1, \dots, A_r the corresponding APFs.

Two-sample test

- D_0 and E_0 : two independent random rotated and rescaled persistence diagrams.
- First sample is r_1 IID copies of D_0 : D_1, \dots, D_{r_1} .
- Second sample is r_2 IID copies of E_0 : E_1, \dots, E_{r_2} .
- $r = r_1 + r_2$ and A_1, \dots, A_r the corresponding APFs.
- **Aim:** Test $\mathcal{H}_0: D_0 = E_0$.

Two-sample test

- D_0 and E_0 : two independent random rotated and rescaled persistence diagrams.
- First sample is r_1 IID copies of D_0 : D_1, \dots, D_{r_1} .
- Second sample is r_2 IID copies of E_0 : E_1, \dots, E_{r_2} .
- $r = r_1 + r_2$ and A_1, \dots, A_r the corresponding APFs.
- **Aim:** Test $\mathcal{H}_0: D_0 = E_0$.
- \overline{A}_{r_1} and \overline{A}_{r_2} : the empirical mean of A_1, \dots, A_{r_1} and $A_{r_1+1}, \dots, A_{r_1+r_2}$.
- $0 \leq T_1 < T_2 < \infty$.
- $KS_{r_1, r_2} = \sqrt{\frac{r_1 r_2}{r_1 + r_2}} \sup_{m \in [T_1, T_2]} |\overline{A}_{r_1}(m) - \overline{A}_{r_2}(m)|$.

Two-sample test

- D_0 and E_0 : two independent random rotated and rescaled persistence diagrams.
- First sample is r_1 IID copies of D_0 : D_1, \dots, D_{r_1} .
- Second sample is r_2 IID copies of E_0 : E_1, \dots, E_{r_2} .
- $r = r_1 + r_2$ and A_1, \dots, A_r the corresponding APFs.
- **Aim:** Test \mathcal{H}_0 : $D_0 = E_0$.
- \overline{A}_{r_1} and \overline{A}_{r_2} : the empirical mean of A_1, \dots, A_{r_1} and $A_{r_1+1}, \dots, A_{r_1+r_2}$.
- $0 \leq T_1 < T_2 < \infty$.
- $KS_{r_1, r_2} = \sqrt{\frac{r_1 r_2}{r_1 + r_2}} \sup_{m \in [T_1, T_2]} |\overline{A}_{r_1}(m) - \overline{A}_{r_2}(m)|$.
- Large values are critical for \mathcal{H}_0 .
- Problem: the asymptotic distribution of KS_{r_1, r_2} known but intractable.
⇒ Bootstrap procedure.

Theorem

Assume that $\lambda \in (0, 1)$ such that $r_1/r \rightarrow \lambda$ as $r \rightarrow \infty$. Under mild conditions, using a bootstrap method where we resample B times,

- if \mathcal{H}_0 is true,

$$\lim_{r \rightarrow \infty} \lim_{B \rightarrow \infty} \mathbb{P} \left(KS_{r_1, r_2} > \hat{q}_\alpha^B \right) = \alpha,$$

- if \mathcal{H}_0 is not true and $\sup_{m \in [T_1, T_2]} |\mathbb{E} \{ A_{D_0} - A_{E_0} \} (m)| > 0$,

$$\lim_{r \rightarrow \infty} \lim_{B \rightarrow \infty} \mathbb{P} \left(KS_{r_1, r_2} > \hat{q}_\alpha^B \right) = 1.$$

Example: Brain artery trees dataset (Bendich *et al.*, 2016)

- Subjects: 46 women and 49 men. Each subject/tree graph has $\approx 10^5$ nodes.
- Bendich *et al.* (2016) wanted to capture how the arteries bend through space and to detect age and gender effects.
- The age effect was clearly revealed \Rightarrow we focus on the gender effect.



Another example: Brain artery trees

Bendich *et al.* (2016) performed a permutation test based on the mean of the 100 largest lifetimes of each subject:

- When $k = 0$ (connected components), p -value of 10%.
- When $k = 1$ (holes), p -value of 3%.

Another example: Brain artery trees

Bendich *et al.* (2016) performed a permutation test based on the mean of the 100 largest lifetimes of each subject:

- When $k = 0$ (connected components), p -value of 10%.
- When $k = 1$ (holes), p -value of 3%.

We distinguish between male and female subjects using our two-sample test statistic KS_{r_1, r_2} based on APF_{kS} .

Another example: Brain artery trees

Bendich *et al.* (2016) performed a permutation test based on the mean of the 100 largest lifetimes of each subject:

- When $k = 0$ (connected components), p -value of 10%.
- When $k = 1$ (holes), p -value of 3%.

We distinguish between male and female subjects using our two-sample test statistic KS_{r_1, r_2} based on APF_{kS} .

- We consider two settings:
 - (A) We use only the 100 largest lifetimes as in Bendich *et al.* (2016).
 - (B) We use all topological features.

Example - Brain artery trees

Estimated p -values of the two-sample test statistic KS_{r_1, r_2} :

	APF ₀		APF ₁	
	$I = [0, 137]$	$I = [0, 60]$	$I = [0, 25]$	$I = [15, 25]$
Setting (A)	5.26	3.26	3.18	2.72
Setting (B)	7.67	3.64	20.06	1.83

- As in Bendich *et al.* (2016): Usually better results when $k = 1$ (holes). In comparison with Bendich *et al.* (2016), we see a very clear gender effect.
- Good detection when $k = 0$ (connected components). In contrast to Bendich *et al.* (2016), we see a clear gender effect.
- Problem with APF₁ on $I = [0, 25]$ partly due to outliers (further studies required).

Conclusions:

- We have introduced a new functional summary statistics (the APF) as an alternative to the persistence diagram. It is 1D and usually \leftrightarrow persistence diagram.

Conclusions:

- We have introduced a new functional summary statistics (the APF) as an alternative to the persistence diagram. It is 1D and usually \leftrightarrow persistence diagram.
- We have successfully used it in various situations.

Conclusions:

- We have introduced a new functional summary statistics (the APF) as an alternative to the persistence diagram. It is 1D and usually \leftrightarrow persistence diagram.
- We have successfully used it in various situations.
- E.g. in connection to the extreme rank envelope test and the corresponding plot.

Conclusions:

- We have introduced a new functional summary statistics (the APF) as an alternative to the persistence diagram. It is 1D and usually \leftrightarrow persistence diagram.
- We have successfully used it in various situations.
- E.g. in connection to the extreme rank envelope test and the corresponding plot.
- We have detected a gender effect for the brain artery trees dataset.

Conclusions:

- We have introduced a new functional summary statistics (the APF) as an alternative to the persistence diagram. It is 1D and usually \leftrightarrow persistence diagram.
- We have successfully used it in various situations.
- E.g. in connection to the extreme rank envelope test and the corresponding plot.
- We have detected a gender effect for the brain artery trees dataset.

Perspectives:

- Define new spatial point process models based on their persistence diagrams.
- Use voids ($k = 2$) to study brain artery trees.

Paper available at [arXiv:1611.00630](https://arxiv.org/abs/1611.00630).

Thank you for your attention.